

AWARD NUMBER: W81XWH-12-1-0556

TITLE: Imaging Prostate Cancer Microenvironment by Collagen Hybridization

PRINCIPAL INVESTIGATOR: Martin Pomper MD, PhD

CONTRACTING ORGANIZATION: Johns Hopkins University
Baltimore, MD 21287

REPORT DATE: December 2016

TYPE OF REPORT: Final

PREPARED FOR: U.S. Army Medical Research and Materiel Command
Fort Detrick, Maryland 21702-5012

DISTRIBUTION STATEMENT: Approved for Public Release;
Distribution Unlimited

The views, opinions and/or findings contained in this report are those of the author(s) and should not be construed as an official Department of the Army position, policy or decision unless so designated by other documentation.

REPORT DOCUMENTATION PAGE

Form Approved
OMB No. 0704-0188

Public reporting burden for this collection of information is estimated to average 1 hour per response, including the time for reviewing instructions, searching existing data sources, gathering and maintaining the data needed, and completing and reviewing this collection of information. Send comments regarding this burden estimate or any other aspect of this collection of information, including suggestions for reducing this burden to Department of Defense, Washington Headquarters Services, Directorate for Information Operations and Reports (0704-0188), 1215 Jefferson Davis Highway, Suite 1204, Arlington, VA 22202-4302. Respondents should be aware that notwithstanding any other provision of law, no person shall be subject to any penalty for failing to comply with a collection of information if it does not display a currently valid OMB control number. **PLEASE DO NOT RETURN YOUR FORM TO THE ABOVE ADDRESS.**

1. REPORT DATE December 2016		2. REPORT TYPE Final Report		3. DATES COVERED 30-SEP-2012 TO 29-SEP-2016	
4. TITLE AND SUBTITLE Imaging Prostate Cancer Microenvironment by Collagen Hybridization				5a. CONTRACT NUMBER W81XWH-12-1-0556	
				5b. GRANT NUMBER PC111750P1	
				5c. PROGRAM ELEMENT NUMBER	
6. AUTHOR(S) Martin G. Pomper, MD, PhD E-Mail: mpomper@jhmi.edu				5d. PROJECT NUMBER	
				5e. TASK NUMBER	
				5f. WORK UNIT NUMBER	
7. PERFORMING ORGANIZATION NAME(S) AND ADDRESS(ES) Johns Hopkins University 3400 N Charles St W400 Wyman Park Bldg Baltimore, MD 21218-2680				8. PERFORMING ORGANIZATION REPORT NUMBER	
9. SPONSORING / MONITORING AGENCY NAME(S) AND ADDRESS(ES) U.S. Army Medical Research and Materiel Command Fort Detrick, Maryland 21702-5012				10. SPONSOR/MONITOR'S ACRONYM(S)	
				11. SPONSOR/MONITOR'S REPORT NUMBER(S)	
12. DISTRIBUTION / AVAILABILITY STATEMENT Approved for Public Release; Distribution Unlimited					
13. SUPPLEMENTARY NOTES					
14. ABSTRACT Small collagen mimetic peptide (CMPs) that mimic the amino acid sequence and three dimensional structure of collagen were shown to have specific binding affinity to type I collagen fibers <i>in vitro</i> and specifically to articular cartilage <i>in vivo</i> . Although the exact mechanism of binding is not known fully, evidence is accumulating that supports the idea that the CMP is binding to partially denatured domains of natural collagen by triple helical hybridization. Here we have tested CMP as a collagen targeting agent to allow imaging of stromal collagens in prostate cancer (PCa). Since CMP binds to unstructured collagen domains more readily, it is expected to exhibit selective affinity to metastatic PCa known to contain processed and denatured collagens. We employed both fluorescent and radiolabeled CMP analogs to image murine models of PCa.					
15. SUBJECT TERMS CMP, collagen mimetic peptide, prostate cancer, stromal collagen, helical hybridization, UV decaging, SPECT, NIRF imaging					
16. SECURITY CLASSIFICATION OF:			17. LIMITATION OF ABSTRACT	18. NUMBER OF PAGES	19a. NAME OF RESPONSIBLE PERSON
a. REPORT	b. ABSTRACT	c. THIS PAGE			USAMRMC
Unclassified	Unclassified	Unclassified	UU	21	19b. TELEPHONE NUMBER (include area code)

Table of Contents

	<u>Page</u>
1. Introduction.....	1
2. Keywords.....	1
3. Accomplishments.....	1
4. Impact.....	14
5. Changes/Problems.....	15
6. Products.....	15
7. Participants & Other Collaborating Organizations.....	18

INTRODUCTION

Small collagen mimetic peptide (CMPs) that mimic the amino acid sequence and three dimensional structure of collagen were shown to have specific binding affinity to type I collagen fibers *in vitro* and specifically to articular cartilage *in vivo*. Although the exact mechanism of binding is not known fully, evidence is accumulating that supports the idea that the CMP is binding to partially denatured domains of natural collagen by triple helical hybridization. Here we have tested CMP as a collagen targeting agent to allow imaging of stromal collagens in prostate cancer (PCa). Since CMP binds to unstructured collagen domains more readily, it is expected to exhibit selective affinity to metastatic PCa known to contain processed and denatured collagens. We employed both fluorescent and radiolabeled CMP analogs to image murine models of PCa.

KEYWORDS

CMP, collagen mimetic peptide, prostate cancer, stromal collagen, helical hybridization, UV decaging, SPECT, NIRF imaging

ACCOMPLISHMENTS

1. Five new CMP analogs were synthesized, radiolabeled and evaluated *in vivo* (aim 3.1).
2. A library of six prostate cancer xenograft lines were evaluated *in vivo* and *ex vivo* for CMP-IRDye800CW binding and MMPsense-680 binding (aim 3.1).
3. Three additional pancreatic cancer xenograft lines were tested to confirm CMP binding trends observed for xenograft growth kinetics.
4. [¹²⁵I]iodotyrosyl-CMP9 was visualized by SPECT-CT and specifically accumulates in skeleton
5. The dual-labeled CHX-A-DTPA-IRDye800CW-CMP is stable *in vivo* and is retained within growing prostate tumor xenografts.

GOALS

1. Synthetic optimization of collagen mimetic peptides for high binding affinity to denatured collagens and collagen undergoing remodeling which simulate microenvironment of metastatic tumors.
2. Demonstrate *ex vivo* and *in vivo* targeting/imaging of malignant PCa mediated by CMP hybridization (Years 2-3, 80% complete).
3. Determination of tumor associated collagen signatures (TACS) for PCa's malignancy level by CMP-mediated imaging methods (Years 2-3, 90% complete).

Year 1: Our proposed milestones in year one included: (1) Dual radio- and fluorescent labeling of CMPs retaining high-affinity ($K_d \leq 10^{-8} M$) and specificity for intact and digested collagen (type I) films, (2) Validation of dual-labeled CMPs that display high affinity and specificity for stromal collagens in frozen PCa xenografts and (3) Measurement of pharmacokinetics and *in vivo* imaging of dual-labeled CMPs in mouse subcutaneous PC-3 xenograft models. Efforts focused on

achieving a biologically stable Collagen Mimetic Peptide (CMP) endowed with both gamma-emitting and fluorescent labels (milestone 1). To that end, we employed several strategies utilizing the previously biologically validated, high affinity basic CMP peptide core (Figure 1), which may contain chelators, covalently bound radioiodine moieties and fluorescent dyes.

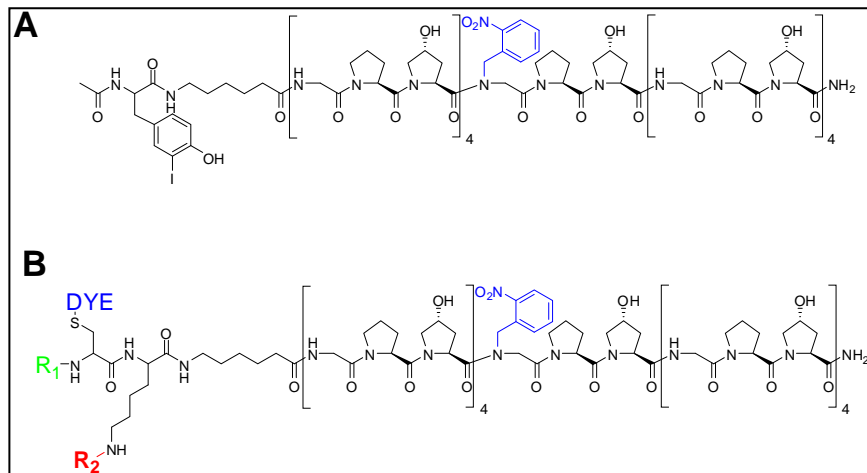


Figure 1. Basic structures of CMPs for radio- and fluorescent dye labeling. Panel (A) shows a photocaged radioiodotyrosyl species with no dye and (B) shows the basic photocaged CMP structure allowing radiolabeling at either lysine 2 or at the amino terminus with chelators for radiometal installment (R_2) or covalent labeling using *p*-iodobenzyl ester (SIB, R_1 or R_2). Cysteine 1 is utilized exclusively for conjugation with maleimide-functionalized dyes.

We first synthesized and tested CMP1, which is depicted in Fig. 1, panel A to determine whether radiolabeled CMPs displayed significantly altered *in vivo* pharmacokinetics and targeting in the absence of a lipophilic near-IR emitting dye. Ahx-CMP₉ was synthesized with an N-terminal tyrosine and was subsequently radiolabeled with I-125 using the Iodogen method. Radiolabeling was nearly quantitative and the resulting peptide was purified using HPLC. Two immunocompetent adult, female CD-1 mice were injected with purified CMP1 with one dose being photodeprotected prior to injection and the other remaining photocaged as a negative control. Figure 2 shows longitudinal SPECT-CT imaging of that pair of mice.

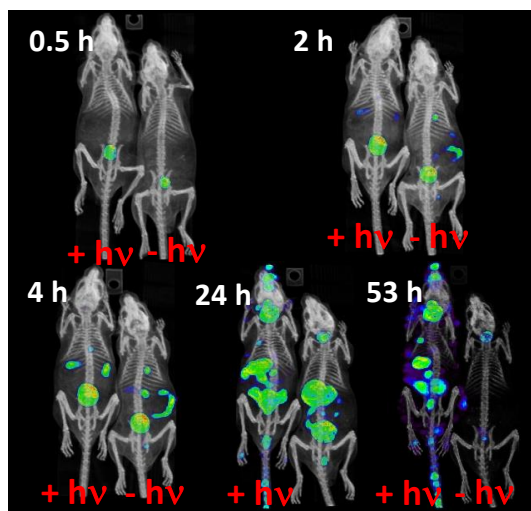


Figure 2. Serial SPECT-CT imaging of CD-1 mice injected with either photodecaged [¹²⁵I]CMP1 (left mouse, + hv) or still-caged CMP1 (right mouse, - hv) at the indicated times. While iodinate tyrosine is a substrate for dehalogenases *in vivo* over time, it is clear that at least some of the photodecaged labeled CMP1 injected into the left mouse remains in the body by 53 hours post-injection and appears to be localized to the spine, rear and forelegs, and possibly nasal cartilage. The mouse on the right retains only metabolized radioiodine accumulated in thyroid and urinary bladder.

Because our aim was to target the soft-tissue collagens of prostate tumors, we performed a dye labeling experiment using either IRDye800CW (LI-COR Biosciences, Lincoln, NE) or IRDye680RD (also LI-COR Biosciences) to confirm pharmacokinetic or targeting differences we began to observe. The IRDye800CW carries a net charge of -3 at physiological pH and is otherwise highly lipophilic. IRDye 680RD carries a net charge of -2 at pH 7.4 and is less lipophilic. We observed that CMPs labeled with IRDye800CW localize primarily to soft tissue collagens and also ossified bone (data not shown) while CMPs labeled with IRDye680RD appear to localize exclusively to articular cartilage within joints (Figure 3).

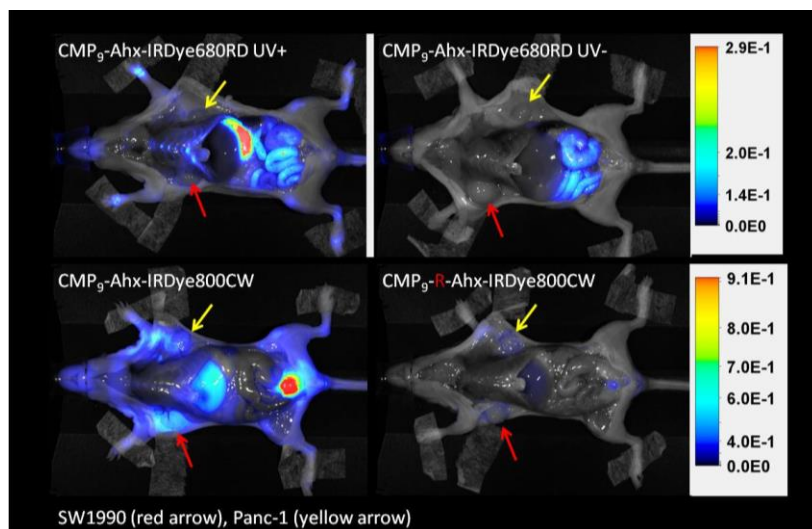


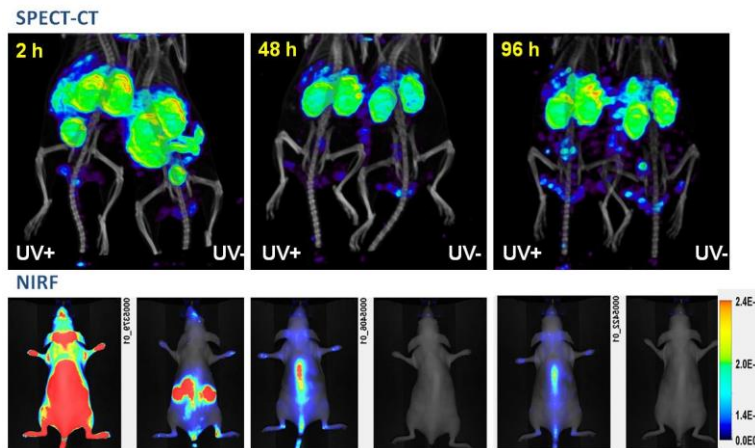
Figure 3. NIRF imaging of tumor-bearing mice with CMPs conjugated to either IRDye680RD or IRDye800CW and imaged at 96 h post-injection. Photodecaged IRDye680RD-conjugated CMP (top left) localizes exclusively to cartilage (wrists, ribs, knees, ankles and toes. GI signal is due to chlorophyll autofluorescence). The same conjugate without photodecaging (top right) does not localize to cartilage or the two subcutaneous tumors (arrows). The mouse injected with photodecaged IRDye800CW conjugate (bottom left) localizes differentially to the tumors (arrows), the surrounding skin, the liver and a

small amount of cartilage uptake in knees and ankles. The control scrambled sequence, decaged IRDye800CW conjugate (bottom right) shows only faint uptake within the tumors and liver, reinforcing CMP binding specificity and apparent dye-mediated selectivity.

With the dye selectivity in mind, we further pursued a dual-modality CMP analog containing the dye of choice (we began with IRDye680RD for targeting ease (cartilage) in normal mice). We began with a NHS ester activated benzyl-bridged DTPA chelator, which is easily conjugated to the free epsilon amine of lysine 2 in Fig. 1B because DTPA will bind In-111 with high affinity and is reported to retain the indium *in vivo* without requiring acidic and heated conditions to chelate the metal. This DTPA, IRDye680RD CMP conjugate (CMP2), was successfully synthesized and purified by HPLC by M. Yu's personnel and was radiolabeled in 100 μ M NaOAc, pH 5 for 30 minutes at room temperature with [111 In]InCl₃ (Nordion Inc., Ottawa ON). Following purification by mini-dialysis (Pierce, MWCO 2000) in PBS, pH 7.5 over 1 h at room temperature, the radiochemical yield was > 90%. Radiochemical purity was assessed by analytical HPLC and was > 95%. Four equivalents of cysteine were added to the formulated [111 In]CMP2 in PBS. Two mice were injected with this formulation where one mouse received photodeprotected [111 In]CMP2 and the other mouse received still-caged [111 In]CMP2 negative control. The mice were then serially scanned using SPECT-CT and NIRF imaging (Figure 4). That experiment revealed that the CMP2 was binding to cartilage as expected but only in the fluorescence images. The SPECT-CT scans showed only kidney with a small amount of liver uptake and little uptake in spine. This suggested that the DTPA chelator may not be able to strongly chelate the In-111 *in vivo* over the relatively long 96 hour uptake period.

Next, a p-benzyl-isothiocyanate bridged DOTA conjugate was made to substitute for the DTPA (position R2 in Figure 1B) as a higher affinity chelator (Figure 5, CMP3), which will resist transchelation *in vivo*, resulting in a biologically stable dual-labeled peptide. CMP3 was successfully synthesized and purified by HPLC prior to radiolabeling.

Figure 4. Serial SPECT-CT and NIRF imaging of dual-labeled $[^{111}\text{In}]\text{CMP2}$. Photodecaged tracer (UV+) and still-caged (UV-) tracer injected mice are shown. NIRF imaging (lower panels) clearly demonstrate the expected cartilage-targeted binding by the decaged tracer only (spine) while the SPECT-CT imaging does not replicate this pattern. The SPECT-CT images show primarily renal excretion and possibly binding since that uptake persists out to 96 h post-injection.



Radiolabeling with $[^{111}\text{In}]\text{InCl}_3$ occurred in 100 μM NaOAc buffer

with heating to 45° C for one hour. Free In-111 was removed by microdialysis cassette against PBS, pH 7.5 for 1 hour. Radio TLC was used to assess radiochemical purity before and after a test-decaging. The presence of multiple radioactive spots after photodecaging suggested liberation of both radiometal, possibly caused by the presence of reductive cysteine quench. The 0.25 equivalents of cysteine added to the vehicle during CMP formulation for injection is to react with and detoxify the resultant benzyl aldehyde produced during decaging. Nevertheless, CMP3 was tested in two normal SKH mice, who were imaged using both SPECT-CT and NIRF imaging to track both the radiolabel and the fluorescent CMP. Figure 5 shows the CMP structure and imaging results.

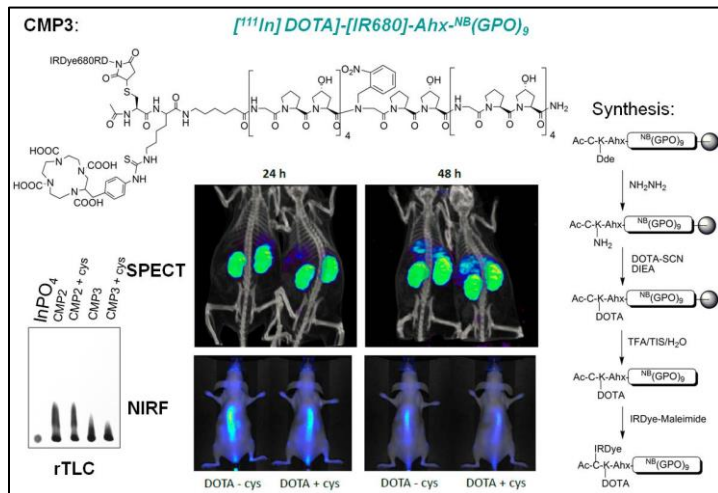


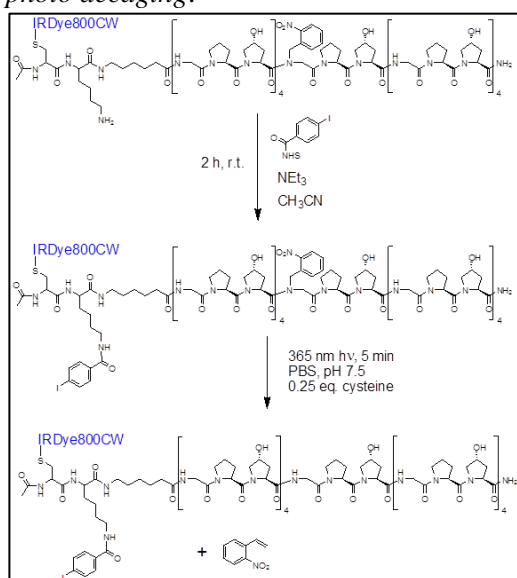
Figure 5. CMP3 structure, synthesis, radio TLC and *in vivo* imaging results. Radio TLC in bottom left shows multiple labeled species following photodeprotection in the presence and absence of cysteine. The DTPA conjugated (CMP2 in lanes 2 and 3) migrate further than CMP3 conjugates, likely reflecting a net -1 charge on CMP2. Spots at the origin may be free radiometal or may represent non-migratory autotriplex CMP following photodecaging.

Conclusions Year 1: The fluorescent imaging consistently showed skeletal targeting with the IRDye680RD dual-labeled conjugates and always after decaging and with targeted peptide (ie not scrambled sequence). The SPECT-CT imaging with radioindium-containing chelator conjugates showed no observable evidence of skeletal cartilage targeting despite concomitant NIRF imaging showing fluorescent targeting. This suggested the radiometal is likely being liberated prior to or immediately after injection. Because photocaged CMPs must be deprotected with intense UV light for 5 minutes and that process generates heat, one hypothesis was the heat from decaging (or from thermal melting in uncaged, triplex CMP) coupled with the relatively high pH of PBS (the vehicle used for mouse injections) liberated a significant portion of both DTPA and DOTA-chelated radioindium complex, which is also suggested by the radio TLC data.

Labeling with radioiodine, however, provided evidence of some success with SPECT-CT imaging that is also consistent with concomitant fluorescent imaging. Labeling with N-acetylated iodotyrosine (CMP1) provided sharp contrast between targeted CMP and scrambled sequence CMP by 53 hours post-injection. While iodotyrosine is a biological substrate for dehalogenases, *p*-iodo-benzoylamide (SIB) is not.

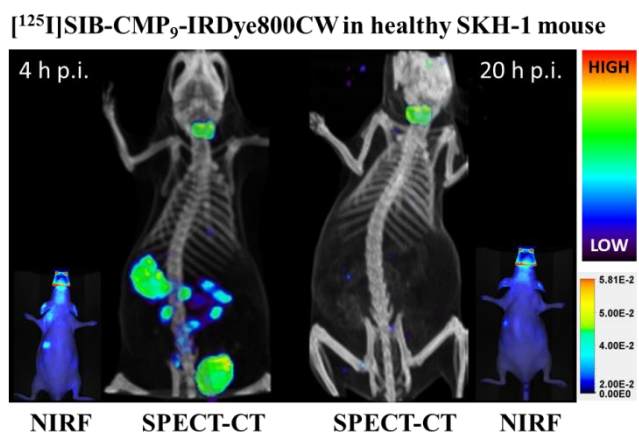
Year 2: In year two, we synthesized several mono- and dual-labeled CMP analogs and tested them *in vivo* for their pharmacokinetic profiles. As we observed what appears to be widespread metabolism in each analog, we have continued our efforts to install and retain a radionuclide label to allow for tomographic and translatable *in vivo* studies of the tumor microenvironment. Our approach has centered on placing a lysine residue C-terminal to a cysteine residue directly conjugated to a bulky IRDye through a maleimide-thiol linkage. **Scheme 1** shows conjugation of [¹²⁵I]SIB-NHS ester to the lysyl-CMP-IRDye scaffold. Para-iodo-benzoyl amide linkages are both chemically and biologically robust and this analog was expected to perform well *in vivo*.

Scheme 1. Conjugation of [¹²⁵I]SIB to Ac-C(IRDye800CW)-K-CMP₉-CONH₂ and photo decaging.



In vivo testing of this dual-modality compound utilizing both SPECT-CT and near IR fluorescence imaging (NIRF) revealed that both the radioiodine label was quickly metabolized and the CMP scaffold performed poorly as shown in **Figure 6**. We speculate that the use of acetonitrile and triethylamine, vital for deprotonating the epsilon amine of the lysine and solubilizing the SIB group, may have chemically degraded the CMP and perturbed the structure of the dye. A color change in the CMP solution after purification supports alteration of the dye structure.

Figure 6. SPECT-CT and NIRF imaging of [¹²⁵I]SIB-CMP₉ in a healthy SKH-1 mouse.



At 4 hours post-injection, extensive free radioiodine uptake is observed in stomach, GI and thyroid while NIRF imaging shows stomach uptake without characteristic kidney uptake. By 20 hours post-injection, virtually all SPECT and NIRF signals have cleared except for thyroid retention of radioiodine.

Previous attempts to stably dual-label using In-111 nuclide met without success and we tried a simple addition of re-melting the purified labeled solution following photodecaging in case radiometallation resulted in chemical decaging

of the nitrobenzoyl group with resultant refolding. Addition of an 80° C melt step immediately prior to injection into a healthy mouse did improve binding of CMP to skeleton compared with photodecaging alone. **Figure 7** shows the results of this experiment. Because the NIRF imaging showed little of the expected uptake along the spine, which has been previously demonstrated with analogs labeled with IRDye680RD, it would appear that the chemistry and/or purification used to introduce indium may also interfere with the stability of this dye structure.

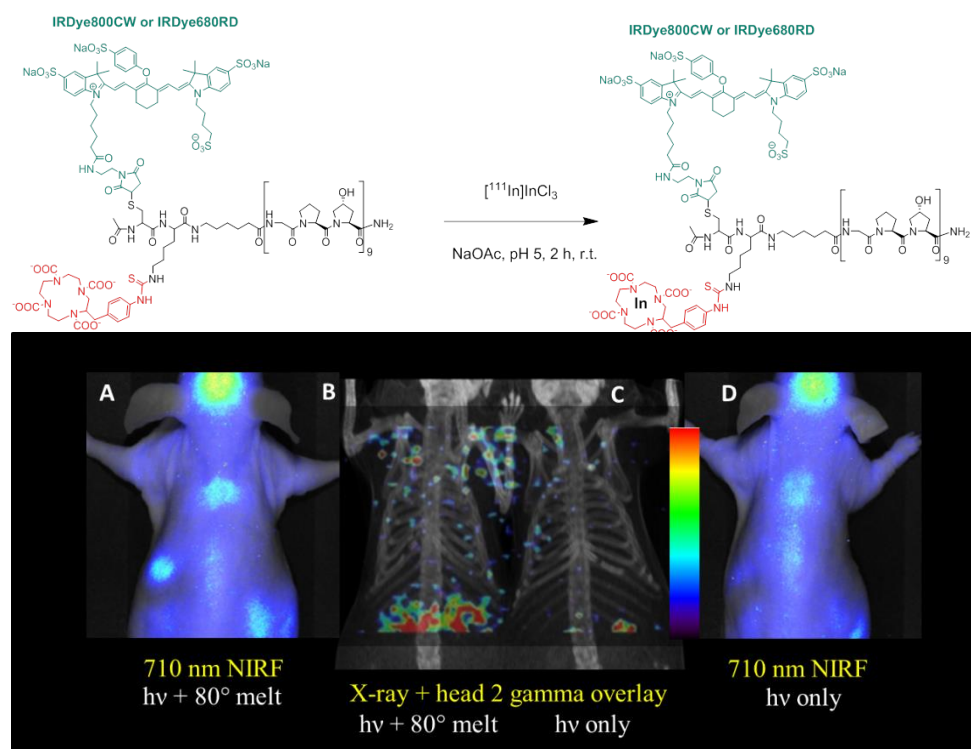


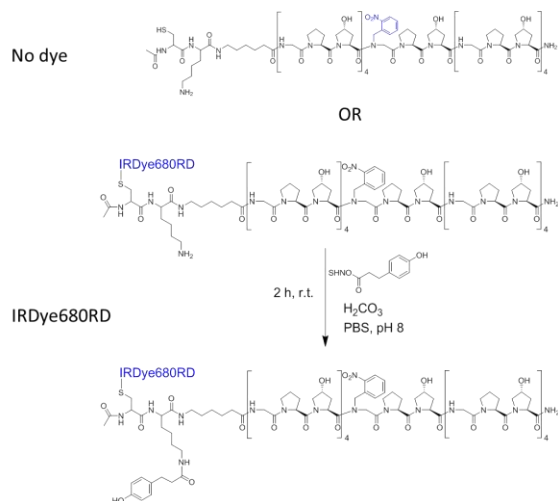
Figure 7. Labeling scheme (top) and in vivo imaging (bottom) of [¹¹¹In]Ac-C-K-CMP₉-CONH₂.

Radiolabeling proceeded with a modest 40% yield followed by a C18 sep-pak purification. A color change was noted following formulation for injection. Planar scintigraphic imaging was performed and overlaid with x-ray and shows more bone uptake

in the photodecaged and melted solution versus decaged only solution. NIRF imaging shows weak uptake in spine, suggesting either perturbation of the IRDye or CMP scaffold.

We then introduced a synthon that is biologically stable and requires gentle, aqueous, pH 8 conjugation conditions to avoid perturbing the IRDye label and nitrobenzoyl cage group. To that effect, we prepared two analogs, Ac-K-CMP₉-CONH₂ and Ac-C-(IRDye680RD)-K-CMP₉-CONH₂, for conjugation with water soluble Bolton-Hunter reagent. Both of these have been prepared according to **Scheme 2** and were easy to label with radioiodine under gentle conditions. These analogs await further chemical and biological characterization.

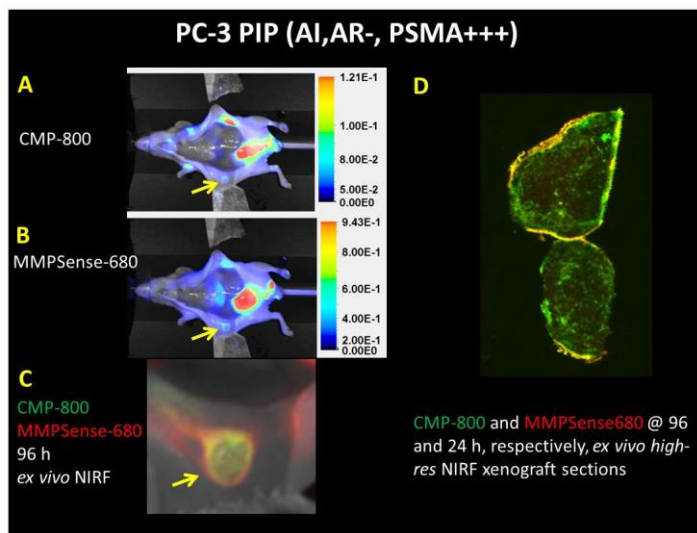
Scheme 2. Conjugation of water soluble Bolton-Hunter reagent to CMPs under aqueous conditions in mild base.



Biological studies proposed under Aim 2 using optically labeled CMP to map collagen remodeling signatures *in vivo* and within a frozen tumor xenograft library were performed with comparison to MMPase activity, which is involved in collagen remodeling. Male athymic nude mice were subcutaneously implanted with a selection of human prostate cancer cell lines to form xenografts ranging from 3.5-7 mm in diameter. Each mouse was intravenously injected with 4 nmol of photodecaged CMP₉-IRDye800CW and 24 h prior to imaging, the mice were also injected intravenously with MMPsense-680™ to concurrently measure the activity of MMPases 2,

3, 9 and 13. As reported in our previously published pilot study (PMID 22927373), CMP uptake overlaps with MMPsense activation but imperfectly. This is expected since cathepsins and other proteases also play large roles in collagen cleavage and remodeling. **Figures 8-12** show both the *in vivo* NIRF imaging of concurrent CMP and MMPsense uptake and the high resolution distributions of both optical probes within representative tumor sections for each xenograft type. CMP distribution was consistent within each cohort of mice with a particular xenograft type and CMP binding was dense and distributed throughout the xenografts of fast-growing tumor lines (PC-3 isoforms) while slower growing xenograft types (DU-145, HP LNCaP) displayed only scattered focal or tumor rim uptake of CMPs. MMPsense uptake was widely and abundantly present in all tumor xenograft lines as well as in the benign but enlarged lymph nodes of mice, where CMP uptake was absent. In essence, CMP uptake correctly distinguished all tumors from enlarged lymph nodes.

Figure 8. Ex vivo NIRF imaging of PC-3 PIP xenograft. AI = androgen independent, AR = androgen receptor negative, PSMA = prostate-specific membrane antigen expression. **A.** CMP₉-IRDye800CW uptake showing tumor uptake (yellow arrow). **B.** MMPsense uptake showing uptake mostly at tumor rim. **C.** A magnified composite of A and B. **D.** High-resolution NIRF imaging of frozen tumor sections with in situ optical probes showing dense CMP accumulation throughout this fast growing xenograft.



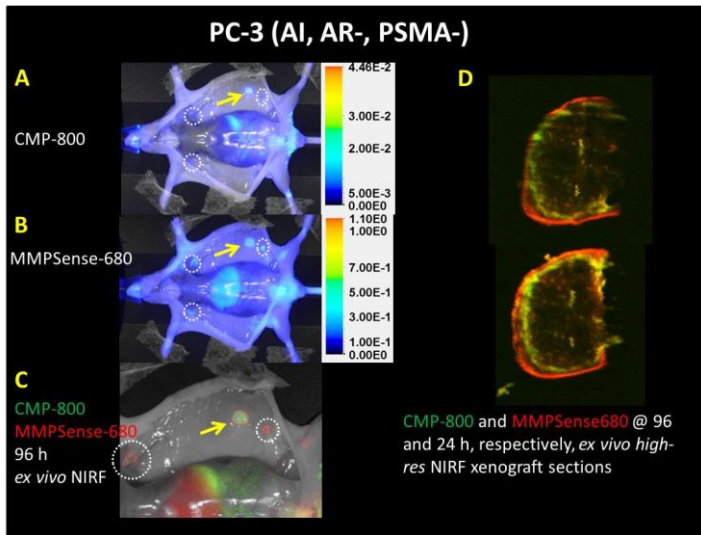


Figure 9. Ex vivo NIRF imaging of PC-3 (wild type) xenograft. Abbreviations and legend exactly as in Fig. 8. Yellow arrow indicates the tumor location. White circles delineate benign lymph nodes that are positive for MMPSense but negative for CMP uptake. High-resolution NIRF imaging of frozen sections (D) with *in situ* optical probes show uptake of CMP (green) throughout the tumor but with increased uptake at the tumor rim. MMPSense (red) uptake is focal throughout the tumor but concentrated at the external edge of the tumor rim.

Figure 10. Ex vivo NIRF imaging of DU-145 xenograft. Abbreviations and legend exactly as in Fig. 3. DU-145 is also AR- (and therefore AI) but is relatively slow growing. **A.** CMP uptake is strongly focal (detail in C) while **(B)** MMPSense uptake is distributed throughout the tumor. This was consistently observed in each DU-145 xenograft studied. **D.** High-resolution NIRF images show the weaker, more focal uptake of CMP (green) in tumor sections while MMPSense (red) uptake is distributed throughout the tumor.

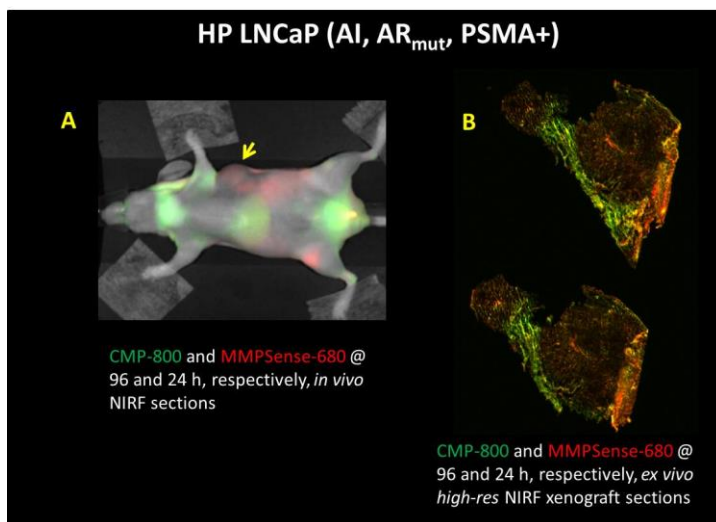
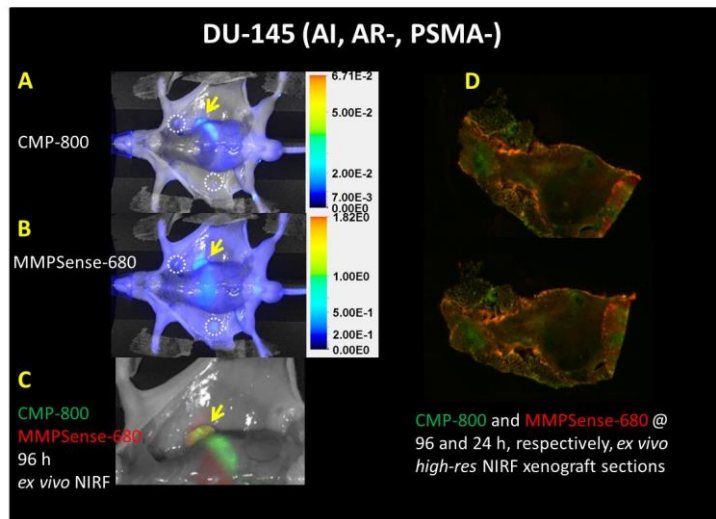


Figure 11. Ex vivo NIRF imaging of HP LNCaP xenograft. AR_{mut} = mutant androgen receptor but androgen insensitive for growth. High passage LNCaP line (JHU isolate) grows relatively slowly as a subcutaneous tumor but has a 100% spontaneous metastasis rate to lymph nodes from this site (manuscript in progress). HP LNCaP tumors are highly hemorrhagic within the tumor and up to 2 cm away in the subcutaneous space. HP LNCaPs only display tumor rim-bound CMPs (green) **(B)** despite intense MMPSense uptake (red) within the tumor and the surrounding site of bruising **(A, red)**.

Finally, we compared CMP and MMPsense distributions of the current prostate cancer library described above with a few pancreatic cancer xenografts grown under the same conditions to ascertain whether CMP uptake and distribution was also correlated to growth kinetics for pancreatic cancer lines. We tested two fast growth (subcutaneous implantation) cell lines (SK1990 and Panc-198) and one slow growth cell line (Panc-1), none of which metastasize spontaneously from this anatomic site. Indeed, CMP uptake was robust and distributed throughout the tumors of the two rapid growth lines (left column, bottom two) while very little CMP accumulation occurred within the slow growth xenograft (top left). This correlates with the CMP uptake patterns observed in the prostate cancer lines. **Table 1** lists quantitative values of CMP distribution among sections and confirms qualitative observations of CMP densities among xenograft types.

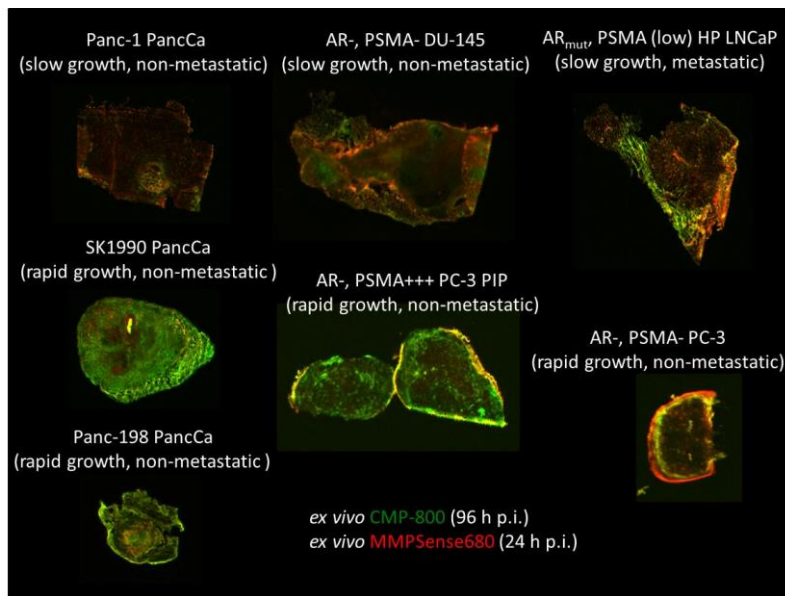


Figure 12. High-resolution NIRF imaging of the prostate cancer library alongside imaging of a few pancreatic cancer xenografts for comparison. Frozen tumor sections with *in situ* optical probes are shown as indicated.

Table 1. Relative optical densities of CMP-800 uptake in tumor xenograft sections.

xenograft line	subQ growth kinetics	O.D. center	O.D. rim/focal ROI
PC-3	rapid	0.25 ± 0.09	1.21 ± 0.40
PC-3 (PSMA+) PIP	rapid	0.26 ± 0.12	NA
DU-145	slow	0.01 ± 0.01	0.06 ± 0.02
HP LNCaP	moderate*	0.03 ± 0.01	0.43 ± 0.18
SW1990	rapid	0.16 ± 0.02	0.23 ± 0.04
Pan-198	moderate	0.08 ± 0.05	NA
Panc-1	slow	0.03 ± 0.02	0.08 ± 0.03

* requires Matrigel to grow; O.D. = optical density of CMP fluorescence

Conclusions for year 2 include chemistry conditions for the conjugation or radiometallation of IRDy-labelled CMPs appear to greatly affect the integrity of the dye and/or the nitrobenzoyl photo cage group. Deviations away from pH 6-8 and heating are to be avoided. Experiments using CMP9-IRDye800CW to map collagen remodeling signatures within mice bearing a range of selected subcutaneous prostate cancer xenografts resulted in the observation of a trend in

which CMP-800 accumulates with higher density in rapidly growing tumors. This trend was also observed in similarly prepared mice bearing subcutaneous xenografts of pancreatic cancer origin.

The concurrent binding of MMPsense™, reporting on the enzymatic activities of MMPs 2, 3, 9 and 13, to each of the tumor models described above revealed no trend in discerning tumor growth kinetics, propensity to metastasize and equally bound to tumor xenografts and benign inflamed lymph nodes while CMP-800 bound to tumors but not benign inflamed lymph nodes.

Year 3: In year three, we focused on two dual-labeled CMP analog that allow for gentle radiolabeling conditions and we tested it *in vivo* for its pharmacokinetic profile in a transgenic and subcutaneous model of PCa. We first tried a follow up SPECT-CT imaging experiment using a dual labeled CMP with [¹²⁵I]SIB and IRDye800CW in a transgenic F1 FVB/TRAMP mouse with severely hypertrophied seminal vesicles. The radiolabeling of this analog is shown in Scheme 1. In healthy mice, this analog rapidly washed out (progress report, year 2). In mice with enlarging, diseased seminal vesicles, this dual labeled CMP bound to the enlarged vesicles and little else as seen by NIRF imaging (Fig. 1A, red). CMP binding overlapped with an inflammation probe that was co-injected (DPA-713-IRDye680LT, green), suggesting the CMP was binding to inflammation-induced tissue remodeling. SPECT-CT imaging of the same animal on the same days as NIRF imaging revealed rapid washout of the CMP from everything except tissue in the lower right quadrant. The SPECT signal remains the same through 24 and 48 hours post-injection, suggesting stable radiotracer accumulation although the SPECT signal does not match the observed fluorescence signal in both inflamed seminal vesicles. This particular analog did not produce matching NIRF and SPECT signal distributions in this model. This supports earlier results showing *in vivo* lability of the radioiodine label despite using the *p*-iodobenzoyl group and the adjacent bulky dye.

Scheme 3. Conjugation of [¹²⁵I]SIB to Ac-C(IRDye800CW)-K-CMP₉-CONH₂ and photo decaging.

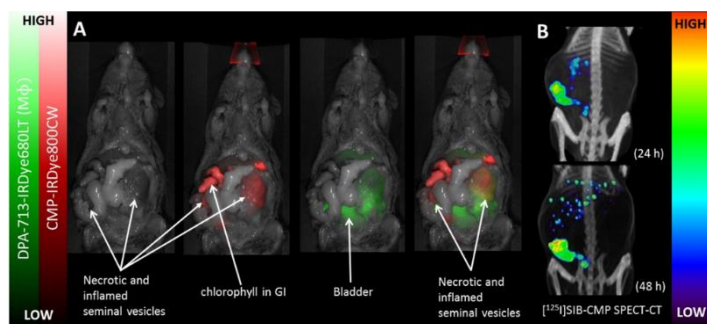
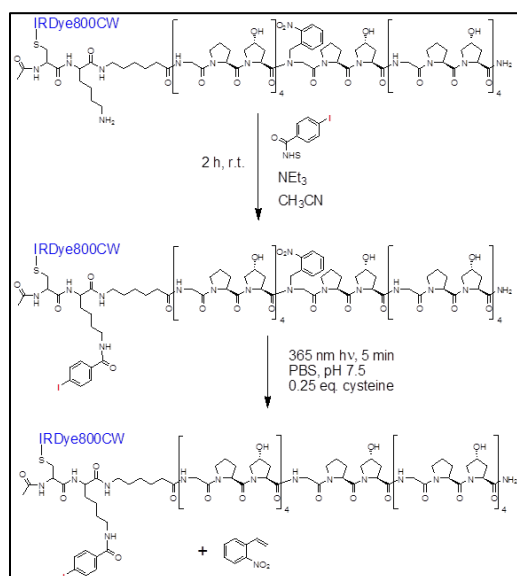
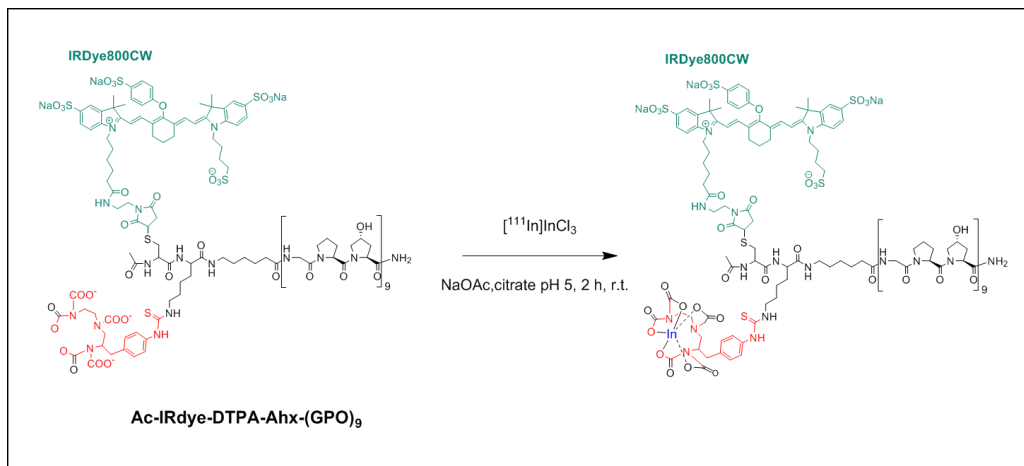


Figure 13. NIRF and SPECT-CT imaging in an F1 TRAMP mouse. A male TRAMP mouse devoid of prostate cancer but containing hypertrophied, inflamed seminal vesicles was scanned using CMP-800CW and an inflammation tracer, DPA-713-IRDye680LT using NIRF imaging. Both inflamed seminal vesicles are displaying CMP uptake (red) co-localizing with the inflammation marker in green. SPECT-CT imaging of the same animal with [¹²⁵I]SIB-CMP shows intense radiotracer uptake at both 24 and 48 h post-injection in the lower right quadrant, possibly representing GI clearance.

In an effort to move away from radioiodine and what appears to be *in vivo* dehalogenase activity, we next synthesized and radiolabeled a dual labeled CMP instilled with both IRDye800CW and CHX-A-DTPA, which chelates In-111 under gentle conditions. Scheme 2 depicts the structure and labeling conditions.

Scheme 4. Radiolabeling of [^{111}In](lys₂)CHX-A-DTPA-(cys₁)IRDye800CW-CMP₉



We then tested this analog in a subcutaneous model of PCa in which mice (n = 4) bore one each of a PC-3 PIP tumor with generally higher

collagen remodeling and one PC-3 flu tumor with less. Figure 2 shows the SPECT-CT images of CMP distribution in the first 6 hours after injection. One mouse was injected with still-caged (inactive) CMP while the remaining four mice were injected with UV-activated labeled CMP. Scant tumor accumulation was observed in the mice until 6 hours after injection. At that time, the PC-3 PIP tumor retained radiotracer signal at the edges of the tumor while the PC-3 flu tumor displayed very little (3D projection and inset). The mouse injected with still-caged CMP displayed very little tumor uptake although had some uptake in the neck. All mice displayed high radiotracer uptake in the liver and kidneys, as it also appears using NIRF detection (data not shown).

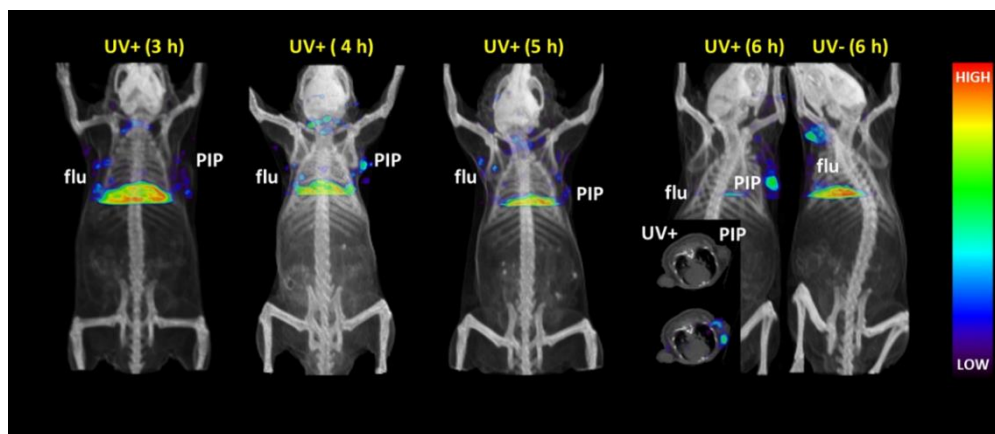


Figure 14. [^{111}In](CXH-A)-(lys₂)-DTPA-CMP₉-(cys₁)-IRDye800CW SPECT-CT at 3-6 h post-injection. Five mice, each bearing a single PC-3 PIP (higher Δ collagen) and PC-3 flu (lower Δ collagen) tumor xenograft, were injected with radiolabeled CMP and imaged by SPECT-CT at the indicated times. PIP tumor uptake of CMP was favored in most mice with the 6 h time point showing clear accumulation of de-caged CMP while still-caged CMP displayed almost no uptake. Liver and renal uptake dominated however (not shown), making tumor uptake appear relatively weak.

At 24 h post-radiotracer injection, higher tumor uptake was apparent in all of the mice except the mouse injected with still-caged (inactive) CMP (Fig. 3). CMP distribution within the tumors was enriched at the edges where growth is occurring. By 24 h, PC-3 flu tumors were also taking up labeled CMP, except in one mouse. Liver and renal uptake of CMP persisted, even in the still-caged CMP mouse, indicating non-specific metabolic excretion in these tissues. This is undesirable and will prompt the pursuit of dye-free CMP analogs as the dye is targeting this excretion pathway.

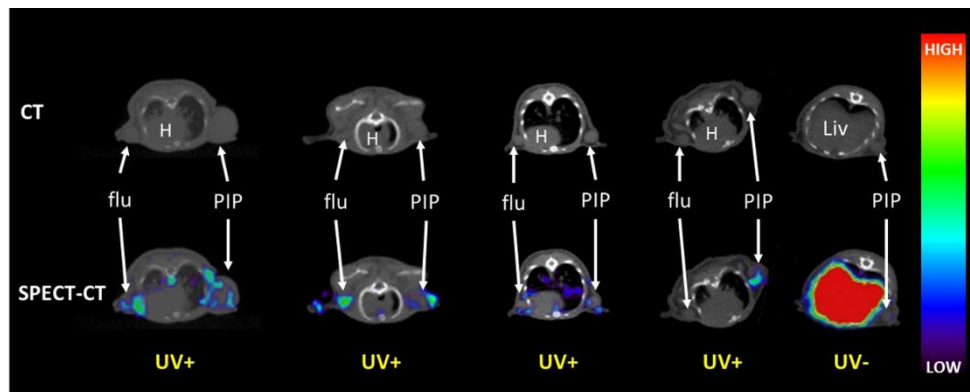


Figure 15. [^{111}In](CXH-A)-(lys₂)-DTPA-CMP₉-(cys₁)-IRDye800CW SPECT-CT at 24 h post-injection. By 24 h post-injection, the same mice in figure 3 displayed stronger CMP uptake at the edges of the tumors, where the tumors are expanding. At this time point, both PC-3 PIP and PC-3 flu tumors are taking up the CMP probe except in the mouse receiving still-caged CMP. “H” represents heart and “Liv” represents liver.

We finished probing the library of PCa xenografts to reflect androgen receptor sensitivity status, expression of the biomarker PSMA and speed at which the tumors were growing. Mice bearing an LAPC4 (AR+, androgen sensitive, PSMA moderate, moderately rapid growth rate) or a C4-2 (AR_{mut}, androgen insensitive, PSMA low, slow growth rate of primary with fast growth rate of local secondary) were injected with a fluorescent-only CMP-IRDye800CW analog followed by MMPsense680 (Perkin Elmer) and the tumors were harvested 72 h (CMP), 24 h (MMPsense) later. Frozen sections of 20 μm thickness were made and scanned using a LI-COR Odyssey scanner. The scans revealed very low CMP uptake in the slow growing primary C4-2 tumor while the fast growing local secondary offshoots displayed CMP binding throughout (Fig. 4, *in vivo* inset and section). MMPsense680 probe showed high MMPase activity in the secondary offshoots but not in the large primary tumor, providing rationale for extracellular matrix remodeling in the secondary tumors where CMP binding is observed.

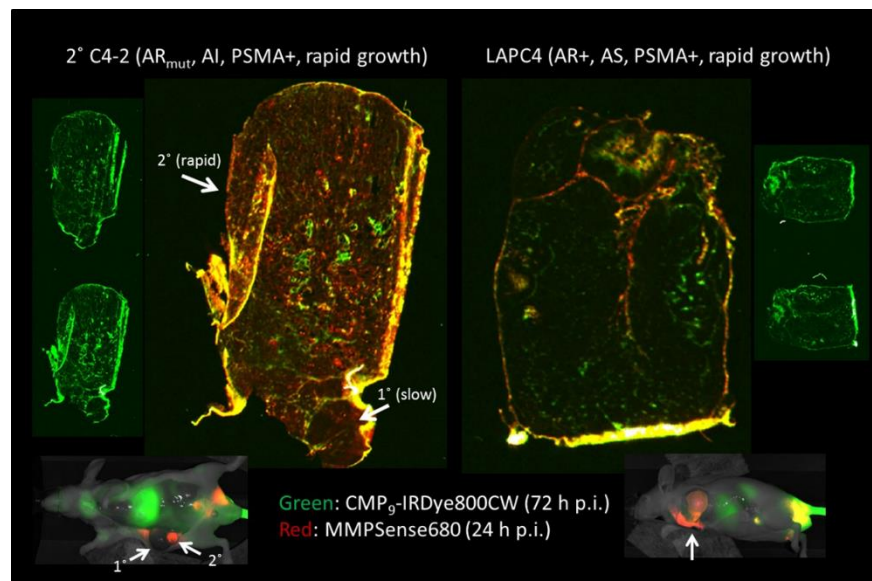


Figure 16. *CMP and MMPsense activity in C4-2 and LAPC4 xenografts.* Athymic nude mice bearing either a slow growing C4-2 xenograft with fast-growing secondary growth or a fast-growing LAPC4 xenograft were injected with 4 nmol of CMP-IRDye800CW and a single dose of MMPsense680. The mice were sacrificed and imaged at 72 h post-CMP and 24 h post-MMPsense. The tumors were then collected, sectioned and imaged to reveal the pattern of CMP distribution relative to MMP activity. Fast-growing tumor tissue took up and retained CMP probe while slow-growing primary C4-2 tissue

took up very little. MMPase activity was prevalent in the fast growing C4-2 nodule as well as the LAPC4 but not the primary C4-2 tissue.

LAPC4 xenografts display a moderately rapid rate of growth and were found to contain a somewhat lower amount of CMP uptake compared with the fast-growing C4-2 secondary tumors. MMPsense uptake was lower than in the secondary C4-2 growths and took on a focal branching pattern, which is also seen in the CMP distribution (green inset). Overall, these uptake patterns in LAPC4 and C4-2 are consistent with the patterns observed for tumor growth rate in the rest of the xenograft library.

We achieved what appeared to be a biologically stable dual-modality CMP but it suffers from high liver and kidney uptake. We have determined that CMP binding does clearly distinguish between tumor and benign enlarged lymph nodes in our mouse model library of xenograft lines. Additionally, CMP uptake appears to distinguish between rapidly growing and slowly growing xenografts while MMPsense probe does not.

Our colleagues in this effort, headed by Michael Yu, have recently determined that CMPs labeled through maleimide linkage with IRDye800CW are especially prone to reverse Michael transconjugation of the dye onto serum protein thiols *in vivo*. This is the reason why CMP conjugates targeted different tissues *in vivo* based on the dye present. Instead of visualizing the remodeling of collagen I *in vivo*, CMP-IRDye800CW conjugates were largely reporting on the distribution of transconjugated serum proteins within the body and PCa tumors.

Conclusions for year 3 include chemistry conditions for the conjugation or radiometallation of IRDy-labelled CMPs appear to greatly affect the integrity of the dye and/or the nitrobenzoyl photocage group. Deviations away from pH 6-8 and heating are to be avoided.

Experiments using CMP9-IRDye800CW to map collagen remodeling signatures within mice bearing a range of selected subcutaneous prostate cancer xenografts resulted in the observation of a trend in which CMP-800 accumulates with higher density in rapidly growing tumors. This trend

was also observed in similarly prepared mice bearing subcutaneous xenografts of pancreatic cancer origin. We finished probing the existing prostate cancer library and have confirmed the trend of CMP binding to growth kinetics to be conserved. Unfortunately, that observed signature within tumors reflects both collagen binding and accumulation of transconjugated dye-labeled serum proteins.

The concurrent binding of MMPSense™, reporting on the enzymatic activities of MMPs 2, 3, 9 and 13, to each of the tumor models described above revealed no trend in discerning tumor growth kinetics, propensity to metastasize and equally bound to tumor xenografts and benign inflamed lymph nodes while CMP-800 bound to tumors but not benign inflamed lymph nodes.

The goal to probe a frozen library of human PCa sections was not performed due to the finding that CMP-IRDye800CW cannot be used *in vivo* due to serum protein side chemistry.

Training and Professional Development

Nothing to report.

Information Dissemination

A publication communicating the reverse Michael transconjugation of CMP-IRDye800CW to serum proteins *in vitro* and *in vivo* has been prepared and submitted to *Molecular Pharmaceutics*.

What do you plan to do during the next reporting period to accomplish the goals?

Nothing to report.

IMPACT

What was the impact on the development of the principal discipline(s) of the project?

While we were ultimately unable to unambiguously map the collagen I remodeling signal *in vivo* within mouse models of prostate cancer due to biochemically unstable dye conjugation *in vivo*, we have since determined that alternative conjugation linkages result in stable labeling *in vivo* although these CMP analogs all report on remodeling within articular cartilage. While this is not particularly pertinent to prostate cancer, it is highly useful in instances of collagen II remodeling in Rheumatoid arthritis and other cartilage-related diseases or wound repair. We did observe trends in the CMP accumulation within different prostate tumor types but they reflect both collagen binding and passive accumulation of transconjugated serum proteins. These observations, in and of themselves, may be useful though not exclusively collagen specific.

What was the impact on other disciplines?

Other groups have been developing collagen hybridizing peptides both as imaging agents and as potential therapeutics.

[Integration of growth factor gene delivery with collagen-triggered wound repair cascades using collagen-mimetic peptides.](#)

Urello MA, Kiick KL, Sullivan MO.
Bioeng Transl Med. 2016 Jun;1(2):207-219.

[Improved Cell Adhesion and Osteogenesis of op-HA/PLGA Composite by Poly\(dopamine\)-Assisted Immobilization of Collagen Mimetic Peptide and Osteogenic Growth Peptide.](#)

Wang Z, Chen L, Wang Y, Chen X, Zhang P.
ACS Appl Mater Interfaces. 2016 Oct 12;8(40):26559-26569.

[Metal Stabilization of Collagen and de Novo Designed Mimetic Peptides.](#)

Parmar AS, Xu F, Pike DH, Belure SV, Hasan NF, Drzewiecki KE, Shreiber DI, Nanda V.
Biochemistry. 2015 Aug 18;54(32):4987-97. doi: 10.1021/acs.biochem.5b00502.

What was the impact on technology transfer?

[Fluorescein-](#) and [biotin-labeled CMP research products](#) developed by the Yu group are now commercially available at Echelon Biosciences.

What was the impact on society beyond science and technology?

Nothing to report.

CHANGES/PROBLEMS

Changes that had a significant impact on expenditures

Nothing to report.

Significant changes in use or care of human subjects, vertebrate animals, biohazards, and/or select agents

Nothing to report.

PRODUCTS

Journal publications:

Lucas L. Benninka, Daniel J. Smitha, Catherine A. Fossb, Martin G. Pomperb, Yang Lia*, and S. Michael Yua* “High Serum Stability of Collagen Hybridizing Peptides” 2016 submitted to *Molecular Pharmaceutics*.

Technologies or techniques

Nothing to report.

Inventions, patent applications, and/or licenses

Provisional Application No. 13/679,431 COLLAGEN MIMETIC PEPTIDES FOR TARGETING COLLAGEN STRANDS FOR IN VITRO AND IN VIVO IMAGING AND THERAPEUTIC USE Filed: November 16, 2012.

Other Products

Nothing to report.

PARTICIPANTS & OTHER COLLABORATING ORGANIZATIONS

What individuals have worked on the project?

Name:	<i>Martin Pomper</i>
Project Role:	<i>Professor</i>
Researcher Identifier (e.g. ORCID ID):	
Nearest person month worked:	<i>1</i>
Contribution to Project:	<i>Planning, strategy, manuscript review</i>
Funding Support:	<i>NIH</i>

Name:	<i>Catherine A. Foss</i>
Project Role:	<i>Assistant Professor</i>
Researcher Identifier (e.g. ORCID ID):	
Nearest person month worked:	<i>4</i>
Contribution to Project:	<i>Dr. Foss performed all in vivo and ex vivo testing of CMP analogs.</i>
Funding Support:	<i>NIH</i>

Has there been a change in the active other support of the PD/PI(s) or senior/key personnel since the last reporting period?

- Martin Pomper

Ended

Title: PSMA-associated PET imaging of CAR T cells

Time Commitments: 0.12 calendar months

Supporting Agency: Juno Therapeutics

Grants Contact: Jake Handy

PI: Pomper

Performance Period: 11/01/2015 – 10/31/2016

Level of Funding:

Description of Goals: To develop a PSMA-based molecular-genetic imaging system for tracking T cells.

Aim 1: Functional assessment of CAR T cells expressing PSMA (full length and truncated versions)

Aim 2: Evaluation of 18F-DCFPyL labelling and tracking of PSMA+ CAR T cells

Title: PSMA Directed Imaging of Prostate Cancer Focus on Androgen Receptor Dynamics

Time Commitments: 2.4

Supporting Agency: NIH/NCI U01CA183031

Grants Contacts: Yantian Zhang; Program Official

PIs: Pomper/Deweese

Performance Period: 11/01/2014-10/31/2016

Level of Funding:

Description of Goals: The overall goal is to validate at least two positron-emitting, PSMA-targeted imaging agents clinically so that they can be used to full advantage in supporting existing and emerging therapies for a spectrum of patients suffering from PCa.

Aim 1. To image treatment-naïve patients with localized-locally advanced primary PCa using DCFBC-PET/magnetic resonance imaging, and correlate signal with that on MR concurrently obtained, as well as with tumor grade, PSMA expression and androgen receptor (AR) signaling before and after two months of neoadjuvant androgen deprivation (ADT).

Aim 2. To image patients with CRPC using DCFBC-PET/MR and correlate findings with bone and soft tissue biopsy.

Aim 3. To image patients with CRPC with DCFBC-PET/MR and correlate with standard 99mTc-based bone scan to guide stereotactic body radiation treatment (SBRT) in patients with oligometastatic disease.

Aim 4. Imaging CRPC with the second-generation, PSMA-targeted PET agent, [18F]DCFPyL.

New

Title: Study to Assess Single and Multiple Intravenous Doses of LY3002813 in Patients

Time Commitments: 0.12 calendar months

Supporting Agency: Shin Nippon Biomedical Laboratories

Grants Contacts: Christopher Hickey, Vice President Business Development

PIs: Pomper

Performance Period: 04/08/16 - 04/07/17

Level of Funding:

Description of Goals: To perform human brain PET imaging as a biomarker to assess the safety, tolerability, pharmacokinetics, and pharmacodynamics of single and multiple intravenous doses

of LY3002813 in patients with mild cognitive impairment due to Alzheimer's disease or mild to moderate Alzheimer's disease

Title: Systemic Radionuclide Therapy Targeted to VEGF Receptors in Tumor Vasculature

Time Commitments: 0.24 calendar months

Supporting Agency: HHSN261201500073C Backer-SIB Tech/ Pomper-JHU)

Grants Contacts: TBN

PIs: Pomper

Performance Period: 09/01/2015 - 05/31/2018

Level of Funding:

Description of Goals: To develop a radiotherapeutic agent that targets VEGF receptors to treat cancer

Title: Plasmid Selection and Characterisation

Time Commitments: 1.20 calendar months

Supporting Agency: Cancer Targeting Systems, Inc.

Grants Contacts: TBN

PIs: Pomper

Performance Period: 02/01/2016 - 07/31/2017

Level of Funding:

Description of Goals: To assess the functionality, yield and specificity of CpG-free and nanoplasmid variants of the CTS construct (backbone_PEG-3-HSV1-tk) to inform and hence enable selection of the optimal variant for further development, suitable for use on the clinic and to provide characterization data.

What other organizations were involved as partners?

Organization Name: The University of Utah

Location of Organization: *Salt Lake City, UT*

Partner's contribution to the project *Michael Yu, PI: chemical synthesis and design*

Financial support:

In-kind support:

Facilities:

Collaboration *collaboration. U. UT makes the compounds, we test them.*

Personnel exchanges NA

Other: